

# Dynamics of two hardcore interacting particles with different diffusion constants in one dimension

**T. Ambjörnsson**

Department of Chemistry, Massachusetts Institute of Technology. 77 Massachusetts Avenue, Cambridge, MA 02139, USA.

E-mail: [ambjorn@mit.edu](mailto:ambjorn@mit.edu)

**L. Lizana**

Department of Chemical and Biological Engineering, Chalmers University of Technology and Göteborg University, Sweden

E-mail: [lizana@fy.chalmers.se](mailto:lizana@fy.chalmers.se)

**R.J. Silbey**

Department of Chemistry, Massachusetts Institute of Technology. 77 Massachusetts Avenue, Cambridge, MA 02139, USA.

E-mail: [silbey@mit.edu](mailto:silbey@mit.edu)

**Abstract.** We investigate the dynamics of a system of two hardcore interacting particles (the particles cannot pass each other) diffusing in an infinite one-dimensional system. The two particles have different diffusion constants. Exact results for the two-particle conditional probability are obtained for arbitrary initial particle positions, and used to obtain the tagged particle probability density function for particles 1 and 2. Excellent agreement is found with stochastic simulations using the Gillespie algorithm.

## 1. Introduction

Crowding effects are ubiquitous in cells [1] - large macromolecules in cells reduce the diffusion rates of particles, influence the rates of biochemical reactions and bias the formation of protein aggregates [2]. Furthermore, the devices used in nanofluidics are becoming smaller; crowding and interactions effects between particles are therefore of increasing importance also in this field.

An example of a system where crowding is prominent is the diffusion of identical hardcore interacting particles (the particles cannot pass each other) in one dimension, so called single-file diffusion. For single-filing systems the particle order is conserved over time ( $t$ ) resulting in interesting dynamical behavior for a tagged particle, quite different from that of classical diffusion. Examples found in nature are ion or water transport through pores in biological membranes [3], one-dimensional hopping conductivity [4] and channeling in zeolites [5]. Furthermore, in biology there are examples where the fact that particles cannot overtake one another are of importance: for instance, DNA binding proteins diffusing along a DNA chain [6, 7, 8]. Single-file diffusion has also been observed in a number of experimental setups such as in colloidal systems and ring-like constructions [9, 10, 11]. One of the most apparent characteristics of single-file diffusion is that the mean square displacement  $\langle (x_T - x_{T_0})^2 \rangle$  (the brackets denote an average over initial positions of non-tagged particles,  $x_T$  is the tagged particle position and  $x_{T_0}$  is the initial position of the tagged particle) of a tagged particle is proportional to  $t^{1/2}$  for large times in an infinite system with a fixed particle concentration; the probability density function (PDF) of the tagged particle position is Gaussian. The first study showing the  $t^{1/2}$  behavior of the mean square displacement and the fact that the PDF is Gaussian is found in Ref. [12]. Subsequent studies include [13, 14, 15, 16, 17]. The  $t^{1/2}$ -law and Gaussian behavior for long times has proven to be of general validity for identical strongly overdamped particles where mutual passage of the particles is excluded independent of the nature of the interaction [18]. Recently, a generalized central limit theorem was proved for the tagged particle motion [19]. It is interesting to note that a mean square fluctuation that scales as  $t^{1/2}$  also occur for monomer dynamics in a polymer within the Rouse model [20]. We point out that anomalous mean square displacement, i.e.  $\langle (x_T - x_{T_0})^2 \rangle$  is *not* proportional to  $t$ , can occur also due to long waiting times between particle jump events (when the waiting time distribution has a divergent first moment) [21, 22]. However, for such processes the probability density is not Gaussian; the anomalous behavior in single-file systems is *not* due to long waiting time densities but rather due to strong correlations between particles [23].

Although much work has been dedicated to single-file diffusion of identical particles, less work has been dedicated to the problem of diffusion of hardcore particles with different diffusion constants. This type of system could be of interest, for instance, for protein diffusion along a DNA chain (there is a plethora of DNA binding proteins). To our knowledge, the only study investigating this type of single-file system is Ref. [24] where the problem of  $N$  diffusing hardcore interacting particles with different diffusion

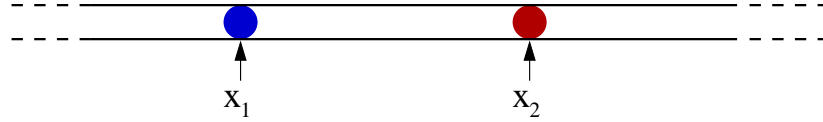


**Figure 1.** Cartoon of the problem considered in this study: two particles are diffusing in a one-dimensional system. Particle  $j$  ( $j = 1, 2$ ) has coordinate  $x_j$ , initial coordinate  $x_{j0}$  and diffusion constant  $D_j$ ; in general  $D_1 \neq D_2$ . The particles cannot overtake, hence at all times we have  $x_1 < x_2$ . In our analytic calculation the system size is assumed to be infinite. In the stochastic simulations we assume a system of finite length  $L$ , with reflecting boundary conditions at  $x = \pm L/2$ .

constants on an infinite line was solved. All the particles were assumed to be initially placed at the *same* position. In this study we extend the results from [24] by solving the problem of diffusion of two hardcore interacting particle with different diffusion constants in which the initial positions for the two particles are *arbitrary*; we provide both an analytic solution as well as results from a stochastic simulation using the Gillespie algorithm. The study of diffusion with arbitrary initial conditions is important in the field of single-file diffusion since in the derivation of the  $t^{1/2}$ -law it is assumed that the particles are initially randomly distributed.

This paper has the following organization: In section 2 we state the problem under consideration and formulate the relevant equations. In section 3 we provide the solution of these equations for the two-particle PDF. In section 4 we integrate out the coordinate for the particle which is not tagged in order to obtain an exact expression for the tagged particle PDF. In section 5 we compare to the results of stochastic simulations using the Gillespie algorithm. The paper is summarized in section 6.

## 2. Problem definition

We consider a system with two hardcore interacting particles diffusing in an infinite one-dimensional system, see figure 1. The particles each have coordinates  $\vec{x} = (x_1, x_2)$  and initial coordinates  $\vec{x}_0 = (x_{10}, x_{20})$ . Due to the hardcore interaction the particles cannot pass each other and therefore retain their order at all times, i.e.

$$-\infty < x_1 < x_2 < \infty. \quad (2.1)$$

We denote the phase-space region spanned by coordinates  $\vec{x}$  satisfying equations (2.1) by  $\mathcal{R}$ . The spatial distribution of the particles as a function of time is contained in the two-particle conditional PDF  $\mathcal{P}(\vec{x}, t | \vec{x}_0)$ . \* This quantity is governed by the 2 + 1 (two coordinates and time) variable diffusion equation

$$\frac{\partial \mathcal{P}(\vec{x}, t | \vec{x}_0)}{\partial t} = \left( D_1 \frac{\partial^2}{\partial x_1^2} + D_2 \frac{\partial^2}{\partial x_2^2} \right) \mathcal{P}(\vec{x}, t | \vec{x}_0), \quad (2.2)$$

\*  $\mathcal{P}(\vec{x}, t | \vec{x}_0) dx_1 dx_2$  gives the probability of particle 1 being in the interval  $[x_1, x_1 + dx_1]$  and particle 2 in  $[x_2, x_2 + dx_2]$  at time  $t$  given that they initially (at time  $t = 0$ ) were at positions  $x_{10}$  and  $x_{20}$  respectively.

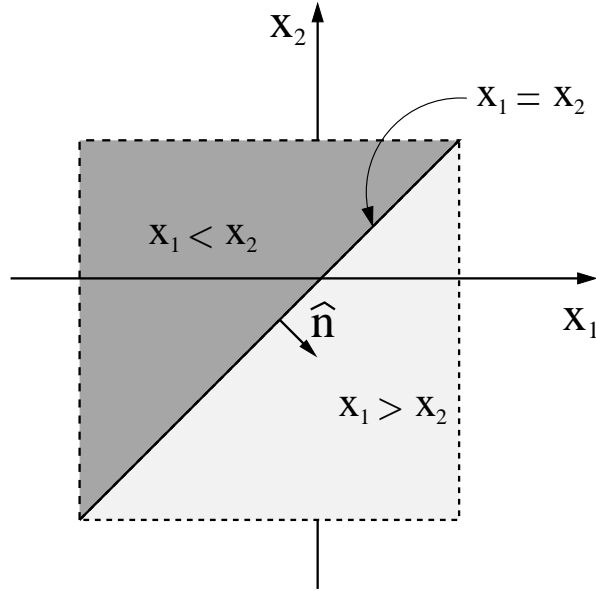


**Figure 2.** Phase space region  $\mathcal{R}$  (the darker upper area,  $x_1 < x_2$ ) for two hardcore interacting particles. For the analytic solutions we assume that  $\mathcal{R}$  extends to minus (plus) infinity for the  $x_1$  ( $x_2$ ) coordinate. In the simulations we impose reflecting conditions at  $x_1 = -L/2$  and  $x_2 = L/2$ , where  $L$  is the length of the system.

for  $\vec{x} \in \mathcal{R}$  [ $\mathcal{P}(\vec{x}, t | \vec{x}_0) \equiv 0$  outside  $\mathcal{R}$ ] and  $D_1$  ( $D_2$ ) is the diffusion constant for particle 1 (particle 2). The initial condition is

$$\mathcal{P}(\vec{x}, 0 | \vec{x}_0) = \delta(x_1 - x_{10})\delta(x_2 - x_{20}) \quad (2.3)$$

where  $\delta(z)$  is the Dirac delta-function. The fact the particles cannot pass each other is described by

$$(D_1 \frac{\partial}{\partial x_1} - D_2 \frac{\partial}{\partial x_2}) \mathcal{P}(\vec{x}, t | \vec{x}_0) |_{x_1=x_2} = 0, \quad (2.4)$$

The above relation is a no flux condition for the normal component of the flux vector across the line  $x_1 = x_2$ , see figure 2: equation (2.2) can be written as a continuity equation  $\partial \mathcal{P} / \partial t = -\vec{\nabla} \cdot \vec{\mathcal{J}}$ , where the flux vector is  $\vec{\mathcal{J}} = -(\hat{x}_1 D_1 \partial \mathcal{P} / \partial x_1 + \hat{x}_2 D_2 \partial \mathcal{P} / \partial x_2)$ , and  $\hat{x}_1$  ( $\hat{x}_2$ ) is a unit vector in the  $x_1$  ( $x_2$ ) direction. The outward normal to the  $x_1 = x_2$  interface is (see figure 2)  $\hat{n} = (\hat{x}_1 - \hat{x}_2) / \sqrt{2}$  which allow us to write equation (2.4) as  $\hat{n} \cdot \vec{\mathcal{J}} |_{x_1=x_2} = 0$ . This reflecting condition guarantees that the probability in the allowed phase-space region  $\mathcal{R}$  is conserved at all times as it should.

### 3. Two-particle probability density function

In order to solve the equations specified in the previous section we make the variable transformation:

$$\begin{aligned} X &= \frac{1}{2} \left( \sqrt{\frac{D_2}{D_1}} x_1 + \sqrt{\frac{D_1}{D_2}} x_2 \right) \\ q &= x_2 - x_1. \end{aligned} \quad (3.1)$$

Equations (2.2), (2.3) and (2.4) then become

$$\begin{aligned} \frac{\partial \mathcal{P}(X, q, t)}{\partial t} &= \left( D^X \frac{\partial^2}{\partial X^2} + D^q \frac{\partial^2}{\partial q^2} \right) \mathcal{P}(X, q, t) \\ \frac{\partial \mathcal{P}(X, q, t)}{\partial q} \bigg|_{q=0} &= 0 \\ \mathcal{P}(X, q, t \rightarrow 0) &= \gamma \delta(X - X_0) \delta(q - q_0) \end{aligned} \quad (3.2)$$

where  $\gamma = (D_1 + D_2)/(2\sqrt{D_1 D_2})$ ,  $X_0 = \sqrt{D_2/D_1}x_{10} + \sqrt{D_1/D_2}x_{20}$  and  $q_0 = x_{20} - x_{10}$  and we introduced the effective diffusion constants

$$\begin{aligned} D^X &= \frac{D_1 + D_2}{4} \\ D^q &= D_1 + D_2 \end{aligned} \quad (3.3)$$

For the case of identical diffusion constants,  $D_1 = D_2 = D$  the equations above express the fact that the relative coordinate  $q$  diffuses with a diffusion constant  $2D$ , whereas the center-of-mass coordinate  $X$  diffuses with a diffusion constant  $D/2$  [25].

Equation (3.2) allows a product solution of the form

$$\mathcal{P}(X, q, t) = \mathcal{P}^X(X, t) \mathcal{P}^q(q, t) \quad (3.4)$$

where

$$\mathcal{P}^X(X, t) = \frac{\gamma}{(4\pi D^X t)^{1/2}} \exp\left(-\frac{(X - X_0)^2}{4D^X t}\right) \quad (3.5)$$

and the solution for  $\mathcal{P}^q(q, t)$  is obtained via the method of images [23] according to

$$\mathcal{P}^q(q, t) = \theta(q) \frac{1}{(4\pi D^q t)^{1/2}} \left( \exp\left(-\frac{(q - q_0)^2}{4D^q t}\right) + \exp\left(-\frac{(q + q_0)^2}{4D^q t}\right) \right) \quad (3.6)$$

where  $\theta(q)$  is the Heaviside step function,  $\theta(q > 0) = 1$  and  $\theta(q < 0) = 0$ . Returning to our original coordinates, equation (3.4), (3.5) and (3.6) become, after some algebraic manipulations:

$$\begin{aligned} \mathcal{P}(\vec{x}, t | \vec{x}_0) &= \theta(x_2 - x_1) \frac{1}{(4\pi D_1 t)^{1/2}} \frac{1}{(4\pi D_2 t)^{1/2}} \\ &\times \left[ \exp\left(-\frac{(x_1 - x_{10})^2}{4D_1 t}\right) \exp\left(-\frac{(x_2 - x_{20})^2}{4D_2 t}\right) \right. \\ &\left. + \exp\left(-\frac{(x_1 - x_{10}^i)^2}{4D_1 t}\right) \exp\left(-\frac{(x_2 - x_{20}^i)^2}{4D_2 t}\right) \right] \end{aligned} \quad (3.7)$$

where the effective image initial positions are

$$\begin{aligned} x_{10}^i &= \frac{D_2 - D_1}{D_1 + D_2} x_{10} + \frac{2D_1}{D_1 + D_2} x_{20} \\ x_{20}^i &= \frac{2D_2}{D_1 + D_2} x_{10} + \frac{D_1 - D_2}{D_1 + D_2} x_{20} \end{aligned} \quad (3.8)$$

Notice that we have  $x_{20}^i - x_{10}^i = -(x_{20} - x_{10})$ , i.e. the distance between the image initial positions is the same as the distance between the initial positions. For  $D_1 = D_2 = D$  we have  $x_{10}^i = x_{20}$  and  $x_{20}^i = x_{10}$  as it should [26]; in contrast, note that for  $D_1 \neq D_2$

the image initial positions depend on  $D_1$  and  $D_2$ . For the case  $x_{10} = x_{20} = 0$  the results above reduce to the results obtained in [24].

It is interesting to compare the above result for  $\mathcal{P}(\vec{x}, t | \vec{x}_0)$  to that of a Bethe-ansatz [27, 28]. It is straightforward to show that equation (3.7) can be written:

$$\begin{aligned} \mathcal{P}(\vec{x}, t | \vec{x}_0) &= \theta(x_2 - x_1) \int_{-\infty}^{\infty} \frac{dk_1}{2\pi} \int_{-\infty}^{\infty} \frac{dk_2}{2\pi} e^{-D_1 k_1^2 t} e^{-D_2 k_2^2 t} e^{-ik_1 x_{10}} e^{-ik_2 x_{20}} \\ &\times [e^{ik_1 x_1} e^{ik_2 x_2} + f(k_1, k_2, x_1, x_2) e^{ik_2 x_1} e^{ik_1 x_2}] \end{aligned} \quad (3.9)$$

where

$$f(k_1, k_2, x_1, x_2) = \exp\left[\frac{D_1 - D_2}{D_1 + D_2}(k_1 + k_2)(x_2 - x_1)\right] \quad (3.10)$$

We note that equation (3.9) has the form of a Bethe ansatz [27], where the ‘‘scattering coefficient’’  $f$  depends on  $x_1$  and  $x_2$  (in the standard Bethe ansatz the scattering coefficient only depends on  $k_1$  and  $k_2$ ); the standard Bethe-ansatz satisfies the equations of motion and the boundary conditions for *fixed*  $k_1$  and  $k_2$ ; in contrast, the solution above does not - it is only after the integrations over  $k_1$  and  $k_2$  are performed [with the appropriate  $x_1$  and  $x_2$  dependent ‘‘mixing’’ of  $k_1$  and  $k_2$  from the 2nd term in equation (3.9)] that the right solution for  $\mathcal{P}(\vec{x}, t | \vec{x}_0)$  is obtained. For the case of identical diffusion constants  $D_1 = D_2 = D$  the mixing of  $k_1$  and  $k_2$  in  $f$  is absent and we have  $f = 1$  in agreement with previous studies [29].

#### 4. Tagged particle probability density

By integrating the two-particle PDF we obtain the tagged particle PDF. The tagged particle probability density (for fixed initial positions) for particle 1 is  $\rho_1(x_1, t | \vec{x}_0) = \int_{x_1}^{\infty} dx_2 \mathcal{P}(\vec{x}, t | \vec{x}_0)$ . Explicitly using equation (3.7) we have:

$$\begin{aligned} \rho_1(x_1, t | \vec{x}_0) &= \frac{1}{(4\pi D_1 t)^{1/2}} \exp\left(-\frac{(x_1 - x_{10})^2}{4D_1 t}\right) \frac{1}{2} \left[1 - \text{erf}\left(\frac{x_1 - x_{20}}{\sqrt{4D_2 t}}\right)\right] \\ &+ \frac{1}{(4\pi D_1 t)^{1/2}} \exp\left(-\frac{(x_1 - x_{10}^i)^2}{4D_1 t}\right) \frac{1}{2} \left[1 - \text{erf}\left(\frac{x_1 - x_{20}^i}{\sqrt{4D_2 t}}\right)\right] \end{aligned} \quad (4.1)$$

where  $\text{erf}(z) = (2/\sqrt{\pi}) \int_0^z dy \exp(-y^2)$  is the error function [30] and  $x_{10}^i$  and  $x_{20}^i$  are given in equation (3.8). Similarly for particle 2 we have that the tagged particle probability density function  $\rho_2(x_2, t | \vec{x}_0) = \int_{-\infty}^{x_2} dx_1 \mathcal{P}(\vec{x}, t | \vec{x}_0)$  becomes

$$\begin{aligned} \rho_2(x_2, t | \vec{x}_0) &= \frac{1}{(4\pi D_2 t)^{1/2}} \exp\left(-\frac{(x_2 - x_{20})^2}{4D_2 t}\right) \frac{1}{2} \left[1 + \text{erf}\left(\frac{x_2 - x_{10}}{\sqrt{4D_1 t}}\right)\right] \\ &+ \frac{1}{(4\pi D_2 t)^{1/2}} \exp\left(-\frac{(x_2 - x_{20}^i)^2}{4D_2 t}\right) \frac{1}{2} \left[1 + \text{erf}\left(\frac{x_2 - x_{10}^i}{\sqrt{4D_1 t}}\right)\right] \end{aligned} \quad (4.2)$$

The quantity  $\rho_j(x_j, t | \vec{x}_0) dx_j$  gives the probability that particle  $j$  is at a position between  $x_j$  and  $x_j + dx_j$ , independently of the position of the other particle, for fixed initial positions  $x_{10}$  and  $x_{20}$ . One may also be interested in the ensemble-averaged tagged particle PDF  $\bar{\rho}_j(x_j, t | x_{j0})$  where, in addition, the initial position of the non-tagged particle has been averaged over; this quantity is calculated in Appendix A. We point out

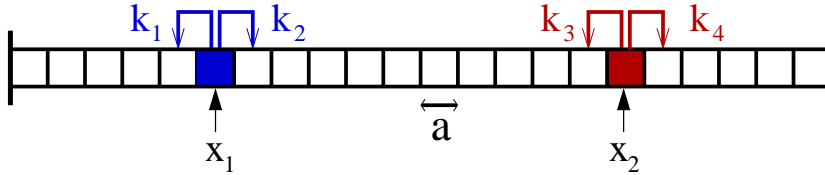


**Figure 3.** Schematic illustration of the lattice on which particles jump in the Gillespie simulation. The number of lattice sites are denoted by  $M$  and the lattice spacing is  $a$ . Particle 1 jump to the left (right) with rate  $k_1$  ( $k_2$ ). Particle 2 jumps to the left (right) with rate  $k_3$  ( $k_4$ ). Note that these rates change during the simulation: if particle 1 is at the leftmost site then we impose the reflecting condition  $k_1 = 0$ . Similarly if particle 2 is at the rightmost site we have  $k_4 = 0$ . If two particles are at neighboring site we set  $k_2 = k_3 = 0$  due to the hardcore repulsion. For the remaining configurations we have  $k_1 = k_2 = k_{\text{free},1}$  and  $k_3 = k_4 = k_{\text{free},2}$ .

that it is only in the limit of a large number of identical hardcore interacting particles that  $\bar{\rho}_j(x_j, t|x_{j0})$ , for a center particle, is a Gaussian with a width that scales with time as  $t^{1/2}$  (see Introduction). The expression for  $\bar{\rho}_j(x_j, t|x_{j0})$  ( $j = 1, 2$ ) given in Appendix A does *not* give a scaling law  $\langle (x_j - x_{j0})^2 \rangle \sim t^{1/2}$ . It remains a challenge to generalize the results in this study to a large number of particles with different diffusion constants, and investigate how the  $t^{1/2}$ -law for the case of identical particles is modified.

## 5. Stochastic simulations

In this section we perform stochastic simulations in order to validate the analytic results in the previous sections. Furthermore, the stochastic simulations allow us to investigate how the diffusion changes if the system size is made *finite* with reflecting conditions at the ends (all analytic results of the previous sections are valid only for an infinite system).

Stochastic simulations using the Gillespie algorithm [31, 32, 33] is a convenient technique for generating stochastic trajectories for interacting particles. Briefly, (in a similar fashion to Ref. [34]) we consider hopping of two particles on a lattice with  $M$  lattice sites with lattice spacing  $a$ ; the length of the box is hence  $L = Ma$ . The dynamics is governed by the 'reaction' probability density (rPDF)

$$P(\tau, \mu) = k_\mu \exp\left(-\sum_\nu k_\nu \tau\right) \quad (5.1)$$

where  $\tau$  is the waiting time between jumps and  $k_\mu$  are the corresponding jump rates; there are four jump rates for the process considered here: the rate for particle 1 jumping to the left and right is  $k_1$  and  $k_2$  respectively; similarly we denote by  $k_3$  and  $k_4$  the left and right jump rates for particle 2, see figure 3. For the case that the two particles are not neighbors nor are at the end lattice points the two particles diffuse independently and we set  $k_1 = k_2 = k_{\text{free},1}$  and  $k_3 = k_4 = k_{\text{free},2}$ . For the case that particle 1 (particle 2) is at the leftmost (rightmost) lattice point we have the reflecting condition  $k_1 = 0$  ( $k_4 = 0$ ). If two particles are at neighboring sites the hardcore repulsion requires  $k_2 = k_3 = 0$ .

Thus, a stochastic time series is generated through the steps: (1) place the two particles at their initial positions; (2) From the rPDF given in equation (5.1) we draw the random numbers  $\tau$  (waiting time) and  $\mu$  (what particles to move and in what direction) - we use the direct method [31], but there are alternatives [33]; (3) Update the positions  $X_1(t)$  and  $X_2(t)$  of the particles, the time  $t$  and the rates  $k_1, k_2, k_3$  and  $k_4$  for the new configuration and return to (2); (4) The loop (1)-(3) is repeated until  $t \geq t_{\text{stop}}$ , where  $t_{\text{stop}}$  is the stop time for the simulation. This procedure produces a stochastic time series  $X_1(t)$  and  $X_2(t)$  for  $0 \leq t \leq t_{\text{stop}}$ . If steps (1)-(4) are repeated  $n$  times ( $n$  ensembles) one obtains a histogram of particle positions (at specified times). The ensemble average results of a Gillespie time series is equivalent to the solution of a master equation incorporating the rates given above [31, 32]. In the limit  $a \rightarrow 0$  with fixed diffusion constants  $D_1 = k_{\text{free},1}a^2$  and  $D_2 = k_{\text{free},2}a^2$  the master equation approaches the diffusion equation as specified in section 2 for an infinite box. Therefore, the stochastic simulation should agree with the analytic results as obtained in the preceding sections in the  $a \rightarrow 0$  limit (for an infinite box). The main effect of the finite box considered in the simulations (with reflecting conditions) is to modify the the long-time limit (i.e. for  $t \gg L^2/D_j$ ): we should reach the equilibrium PDFs [29, 35]

$$\begin{aligned}\rho^{\text{eq}}(x_1) &= \frac{2}{L^2} \left( \frac{L}{2} - x_1 \right), \\ \rho^{\text{eq}}(x_2) &= \frac{2}{L^2} \left( \frac{L}{2} + x_2 \right)\end{aligned}\tag{5.2}$$

The results given in equation (5.2) is obtained by direct integration of the two-particle equilibrium PDF  $P^{\text{eq}}(x_1, x_2) = 2\theta(x_2 - x_1)/L^2$ , where  $\theta(z)$  is the Heaviside step-function. Notice that the equilibrium results are independent on  $D_1$  and  $D_2$  as it should. In figure 4 we illustrate the result of a Gillespie simulation using  $n = 50000$  ensembles on a lattice with  $M = 500$ , and compare to the PDFs (4.1) and (4.2) as well as the equilibrium PDF (5.2). We notice an excellent agreement within the limit of applicability.

## 6. Summary and outlook

We have in this study investigated the dynamics of two hardcore interacting particles with different diffusion constants diffusing in a one-dimensional system. An exact result for the two particle probability density function (PDF) for arbitrary initial particle positions was obtained and used to derive explicit expressions for the tagged particle PDFs. Our results are in excellent agreement with stochastic simulations using the Gillespie algorithm.

It will be interesting to see whether it is possible to generalize our two-particle results to  $N$  particles with different diffusion constants. In particular, a remaining challenge is to investigate how the scaling of the mean square displacement with time  $t$  differs from  $t^{1/2}$ -scaling valid for the case of identical diffusion constant in the  $N \rightarrow \infty$  limit.

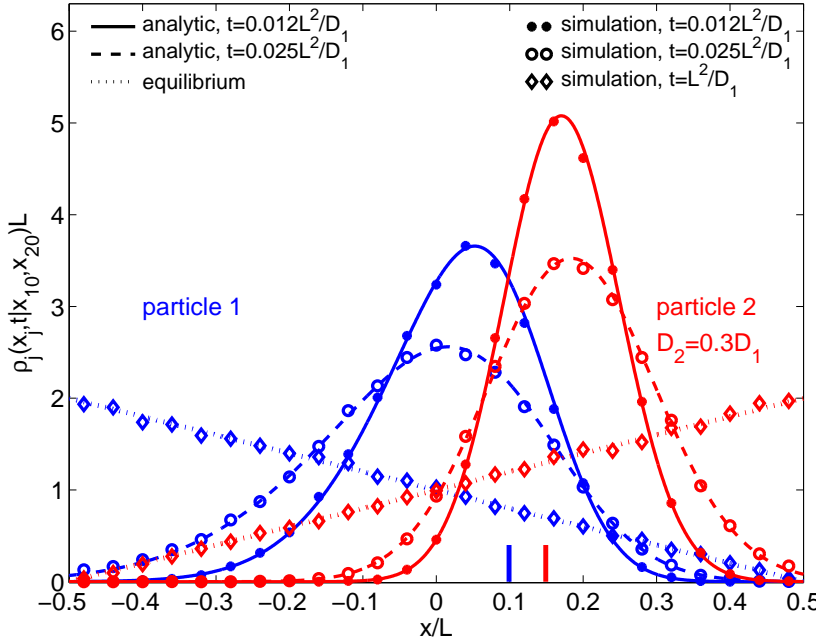


**Figure 4.** Tagged particle PDF  $\rho_j(x_j, t | \vec{x}_0)$  for two hardcore interacting particles ( $j = 1, 2$ ). The solid and dashed blue [red] curves corresponds to the tagged particle PDF for particle 1 [particle 2] at different times as given in equation (4.1) [equation (4.2)]. The ratio of the diffusion constants is  $D_2/D_1 = 0.3$ . The symbols correspond to the results of the Gillespie simulation, ensemble-averaged over  $n = 50000$  ensembles for  $M = 500$  lattice sites; the data was binned into 25 bins. The vertical bars at the bottom of the figure corresponds to the initial positions for the two particles ( $x_{10} = 0.10L$  and  $x_{20} = 0.15L$ ). For long time  $t > L^2/D$  the equilibrium is reached - the dashed lines correspond to the analytic result as given in equation (5.2). Notice the excellent agreement between the stochastic simulation and the analytic results in the regimes of validity.

## Acknowledgments

We are grateful to Ophir Flomenbom for helpful discussions. T.A. acknowledges the support from the Knut and Alice Wallenberg Foundation. Part of this research was supported by the NSF under grant CHE0556268.

## Appendix A. Ensemble averaged tagged particle PDF

Let us consider ensemble averaging the results given in section 4 over the initial particle positions (for the particle which is not tagged). We imagine the particles to be in a box of length  $L$  and assume that  $L$  is “large”; more precisely, we assume that  $L$  is sufficiently large so that the particles have not had time to reach the ends of the box, i.e. we consider times such that  $t \ll L^2/D$ , where  $D$  is the largest of  $D_1$  and  $D_2$ . We can then use the infinite box results from section 4, and we define the ensemble averaged

tagged particle PDFs as

$$\begin{aligned}\bar{\rho}_1(x_1, t|x_{10}) &= f_R \int_{x_{10}}^{L/2} dx_{20} \rho_1(x_1, t|x_{10}, x_{20}), \\ \bar{\rho}_2(x_2, t|x_{20}) &= f_L \int_{-L/2}^{x_{20}} dx_{10} \rho_2(x_2, t|x_{10}, x_{20})\end{aligned}\quad (\text{A.1})$$

where

$$\begin{aligned}f_R &= \frac{1}{L/2 - x_{10}} \\ f_L &= \frac{1}{L/2 + x_{20}};\end{aligned}\quad (\text{A.2})$$

$f_R$  and  $f_L$  are the normalized one-particle initial densities, i.e., we have  $\int_{x_{10}}^{L/2} dx_{20} f_R = 1$  and  $\int_{-L/2}^{x_{20}} dx_{10} f_L = 1$ . Using the results contained in equations (3.7) and (3.8) the conditional PDF for particle 1 becomes:

$$\begin{aligned}\bar{\rho}_1(x_1, t|x_{10}) &= \Psi(x_1, x_{10}, t) \Psi_R^R(x_1, x_{10}, t) + \Omega_R^R(x_1, x_{10}, t) \\ \Psi(x_1, x_{10}, t) &= \frac{1}{(4\pi D_1 t)^{1/2}} e^{-\eta_1^2} \\ \Psi_R^R(x_1, x_{10}, t) &= 1 - \frac{f_R}{2} \sqrt{\frac{4D_1 t}{\pi}} \left\{ \sqrt{\frac{D_2}{D_1}} \exp\left(-\frac{D_1}{D_2} \eta_1^2\right) + \sqrt{\pi} \eta_1 [\text{erf}\left(\sqrt{\frac{D_1}{D_2}} \eta_1\right) + 1] \right\} \\ \Omega_R^R(x_1, x_{10}, t) &= \frac{f_R}{4} \gamma \sqrt{\frac{D_2}{D_1}} \frac{2}{\sqrt{\pi}} \int_{-\infty}^{\eta_1} dy e^{-y^2} \left\{ 1 - \text{erf}\left[\frac{1}{2} \left( \sqrt{\frac{D_1}{D_2}} - \sqrt{\frac{D_2}{D_1}} \right) y + \gamma \eta_1\right] \right\}\end{aligned}\quad (\text{A.3})$$

where  $\eta_1 = (x_1 - x_{10})/(\sqrt{4D_1 t})$  and  $\gamma = (D_1 + D_2)/(2\sqrt{D_1 D_2})$  as before. We have above assumed that  $t \ll L^2/D_1$ . In an identical fashion the conditional PDF for particle 2 becomes:

$$\begin{aligned}\bar{\rho}_2(x_2, t|x_{20}) &= \Psi(x_2, x_{20}, t) \Psi_L^L(x_2, x_{20}, t) + \Omega_L^L(x_2, x_{20}, t) \\ \Psi(x_2, x_{20}, t) &= \frac{1}{(4\pi D_2 t)^{1/2}} e^{-\eta_2^2} \\ \Psi_L^L(x_2, x_{20}, t) &= 1 - \frac{f_L}{2} \sqrt{\frac{4D_2 t}{\pi}} \left\{ \sqrt{\frac{D_1}{D_2}} \exp\left(-\frac{D_2}{D_1} \eta_2^2\right) + \sqrt{\pi} \eta_2 [\text{erf}\left(\sqrt{\frac{D_2}{D_1}} \eta_2\right) - 1] \right\} \\ \Omega_L^L(x_2, x_{20}, t) &= \frac{f_L}{4} \gamma \sqrt{\frac{D_1}{D_2}} \frac{2}{\sqrt{\pi}} \int_{\eta_2}^{\infty} dy e^{-y^2} \left\{ 1 + \text{erf}\left[\frac{1}{2} \left( \sqrt{\frac{D_2}{D_1}} - \sqrt{\frac{D_1}{D_2}} \right) y + \gamma \eta_2\right] \right\}\end{aligned}\quad (\text{A.4})$$

where  $\eta_2 = (x_2 - x_{20})/(\sqrt{4D_2 t})$ , and assuming that  $t \ll L^2/D_2$ . In the limit  $D_1 = D_2 = D$  we can explicitly evaluate  $\Omega_R^R$  and  $\Omega_L^L$  giving the result  $\Omega_R^R = f_R[1 - \text{erf}(\eta_1)][1 + \text{erf}(\eta_1)]/4$  and  $\Omega_L^L = f_L[1 - \text{erf}(\eta_2)][1 + \text{erf}(\eta_2)]/4$ .

[1] Luby-Phelps L 2000 Int. Rev. Cytol. **192** 189.

[2] Ellis R J and Milton A P 2003 Nature **425** 27.

- [3] Hodgkin A L and Keynes R D 1955 *J. Physiol. (London)* **128** 61.
- [4] Richards P M 1977 *Phys. Rev. B* **16** 1393.
- [5] Kukla V, Kornatowski J, Demuth D, Girnus I, Pfeifer H, Rees L, Schunk S, Unger K, and Käger J, 1996 *Science* **272** 702.
- [6] Berg O G, Winter R B and von Hippel P H 1981 *Biochemistry* **20**, 6929.
- [7] Halford S E, Marko J F 2004 *Nucleic Acids Research* **32**, 3040.
- [8] Lomholt M A, Ambjörnsson T and Metzler R 2005 *Phys. Rev. Lett.* **95**, 260603.
- [9] Coupier G, Jean M S and Guthmann C 2006 *Phys. Rev. E* **73** 031112.
- [10] Lutz C, Kollmann M and Bechinger C 2004 *Phys. Rev. Lett.* **92** 026001.
- [11] Wei Q H, Bechinger C, Leiderer P 2000 *Science* **287** 625.
- [12] Harris T E 1965 *J. Appl. Prob.* **2**(2) 323.
- [13] Levitt D G 1973 *Phys. Rev. A* **6** 3050.
- [14] van Beijeren H, Kehr K W and Kutner R 1983 *Phys. Rev. B* **28** 5711.
- [15] Hahn K and Käger J 1995 *J. Phys. A* **28** 3061.
- [16] Arratia R 1983 *Ann. Prob.* **11** 362.
- [17] Aslangul C 1998 *Europhys. Lett.* **44** 284.
- [18] Kollmann M 2003 *Phys. Rev. Lett.* **90** 180602.
- [19] Jara M D and Landim C 2006 *Ann. I.H. Poincaré - PR* **42** 567.
- [20] Shusterman R, Alon S, Gavrinyov T and Krichevsky O 2004 *Phys. Rev. Lett.* **92** 048303.
- [21] Metzler R and Klafter J 2000 *Phys. Rep.* **339** 1.
- [22] Metzler R and Klafter J 2004 *J. Phys. A* **37** R161.
- [23] Rödenbeck C, Käger J and Hahn K 1998 *Phys. Rev. E* **57** 4382.
- [24] Aslangul C 2000 *J. Phys. A* **33** 851.
- [25] Aslangul C 1999 *J. Phys. A* **32** 3993.
- [26] Fisher M E 1984 *J. Stat. Phys.* **34** 667.
- [27] Schütz G M 1997 *J. Stat. Phys.* **88** 427.
- [28] Batchelor M T 2007 *Phys. Today* **60** 36.
- [29] Lizana L and Ambjörnsson T 2008 E-print: arXiv:0801.0563.
- [30] Abramowitz M and Stegun I A *Handbook of Mathematical Functions with Formulas, Graphs, and Mathematical Tables* (Dover, New York, 1964).
- [31] Gillespie D T 1976 *J. Comput. Phys.* **22**, 403.
- [32] Gillespie D T 2001 *J. Chem. Phys.* **115**, 1716.
- [33] Gillespie D T 2007 *Ann. Rev. Phys. Chem.* **58** 35.
- [34] Banik S K, Ambjörnsson T and Metzler R 2005 *Europhys. Lett.* **71** 852.
- [35] Ambjörnsson T and Lizana L, in preparation.